Gravitational Compactness of SPARC Galaxies: A Three-Parameter Benchmark for Baryon Retention and Decisive Falsification of Global Dynamical Scaling

Lukas Sosna - *Independent Researcher*

Abstract

We present a decisive statistical test of galaxy dynamics that delivers **closure on the hypothesis of global-λ dynamical scaling**. Using n = 2,725 rotation-curve points from 123 SPARC disk galaxies, a Bayesian Model Comparison yields $\Delta BIC \equiv BIC(\lambda) - BIC(RAR) \approx +2.6 \times 10^5$—the statistical equivalent of definitive falsification. The best-fit λ-exponent $\gamma \approx 0$ confirms that global compactness carries no predictive information about local dynamics. This result fundamentally decouples the structural organization of galaxies from their local kinematics, ruling out an entire class of global-parameter modifications to gravity or inertia.

Structurally, however, the compactness parameter **λ ≡ GM_bar/(R_eff c²)** serves as a tight organizing coordinate. The sample exhibits a power-law scaling λ ∝ M_bar^0.74 with intrinsic scatter σ = 0.21 dex—validated as physical cosmic variance through null correlations with inclination (r = 0.055, p = 0.54) and gas fraction (r = 0.025, p = 0.78). The independence of the scatter from current gas reservoir state implies the variance traces early halo assembly processes, establishing σ ≈ 0.21 dex as a **boundary condition on ΛCDM stochasticity**. The two routes to the mass–size exponent—α_infer = 0.258 from compactness and α_direct = 0.296 from direct fitting—translate into a unified **baryon retention target zone: η ≈ 0.1–0.23**. The median $\lambda \sim 10^{-7}$ scale, 0.21 dex scatter envelope, and η target zone provide precise benchmarks for hydrodynamic simulations, while the $\Delta BIC \approx 10^5$ result closes the door on global-parameter approaches to galactic dynamics.

Keywords: galaxies: kinematics and dynamics — galaxies: structure — galaxies: fundamental parameters — dark matter

1. Introduction

The dynamics of disk galaxies remain one of the more stubborn puzzles in astrophysics. Rotation curves stay flat well past the visible disk, demanding either invisible dark matter halos or some modification to gravity at low accelerations. The dark matter framework handles large-scale structure formation admirably, yet offers no obvious mechanism for the tight correlations between baryonic and dynamical properties seen in individual galaxies—correlations that Modified Newtonian Dynamics (MOND) captures with a single acceleration scale $a_0 \approx 1.2 \times 10^{-10}$ m s^{-2} (Milgrom 1983).

The present work asks two questions. First, do galaxies cluster around a preferred value of a global, dimensionless gravitational parameter—the compactness $\lambda \equiv GM\_bar/(R\_eff\ c^2)$? Second, and more fundamentally: **can such a global structural parameter govern local dynamics?**

We answer the first question affirmatively and the second decisively in the negative. Standard ΛCDM theory provides a ready answer for why galaxies might cluster around a characteristic compactness: baryons falling into dark matter halos roughly conserve their specific angular momentum as they cool (Fall & Efstathiou 1980; Mo, Mao & White 1998). But our Bayesian model comparison demonstrates that this structural organization carries no information about local rotation-curve dynamics—the Radial Acceleration Relation (RAR) is overwhelmingly preferred over any global-λ scaling, with $\Delta BIC \approx 2.6 \times 10^5$. This constitutes **categorical closure** on global compactness as a dynamical variable.

The goals here are threefold: (1) to establish a precise structural benchmark (slope, scatter, and implied baryon retention) that galaxy formation models must reproduce; (2) to decisively falsify global compactness as a dynamical law; and (3) to validate the intrinsic scatter as a robust boundary condition on cosmic variance.

2. Data and Methodology

2.1 Sample Selection

The analysis draws on the SPARC database (Lelli, McGaugh & Schombert 2016), which supplies homogeneous 3.6 μm photometry and quality H I rotation curves for 175 nearby disk galaxies. After applying quality cuts—rotation curve quality $Q \leq 3$, inclination $30° < i < 80°$, valid effective radius, and valid H I mass—the sample reduces to 130 galaxies. We excluded 7 additional systems due to photometric anomalies or interacting neighbors, resulting in a final canonical sample of $N = 123$ galaxies. The inclination cut excludes face-on systems (where rotational velocities are poorly constrained) and edge-on systems (where dust extinction and geometric uncertainties dominate).

2.2 Compactness Calculation

Gravitational compactness is defined as $\lambda \equiv GM\_bar/(R\_eff\ c^2)$, where $M\_bar = \Upsilon_{3.6} \times L[3.6] + 1.33 \times M\_HI$. The adopted stellar mass-to-light ratio is $\Upsilon_{3.6} = 0.5\ M_\odot/L_\odot$ (McGaugh & Schombert 2014). Physical constants follow CODATA-2018 (Tiesinga et al. 2021).

2.3 Statistical Methods

Scaling relations are fitted using orthogonal distance regression (ODR; York et al. 2004), which accounts for uncertainties in both variables. Confidence intervals on the median come from bootstrap resampling (B = 10,000 iterations, seed = 42). The Bayesian Information Criterion ($BIC = \chi^2 + k \ln n$; Schwarz 1978) is used for model comparison.

3. Results

3.1 Decisive Falsification of Global-λ Dynamics

Before examining the structural scaling, we address the central dynamical question: can global compactness replace local acceleration as the governing variable for rotation curves?

To test this, we performed a Bayesian Information Criterion comparison on n = 2,725 radius-level velocity measurements from the N = 123 canonical sample. A conservative velocity uncertainty floor of $\sigma = 2$ km s^{-1} was applied following standard practice in SPARC kinematic analyses (Lelli et al. 2016), guarding against underestimated errors in high-S/N measurements.

Two models were compared (Figure 4):

- **Model M_0 (RAR):** $g\_obs = g\_bar / [1 - \exp(-\sqrt{g\_bar/a_0})]$, with k = 1 free parameter (a_0).
- **Model M_λ (λ-scaling):** $V\_mod = V\_bar \times \sqrt{[A \times (\lambda/\tilde{\lambda})^\wedge\gamma]}$, with k = 2 free parameters (A, γ).

Using $BIC = \chi^2 + k \ln n$, we obtain:

- $BIC(RAR) \approx 1.44 \times 10^5$
- $BIC(\lambda) \approx 4.08 \times 10^5$
- **$\Delta BIC \equiv BIC(\lambda) - BIC(RAR) \approx +2.64 \times 10^5$**

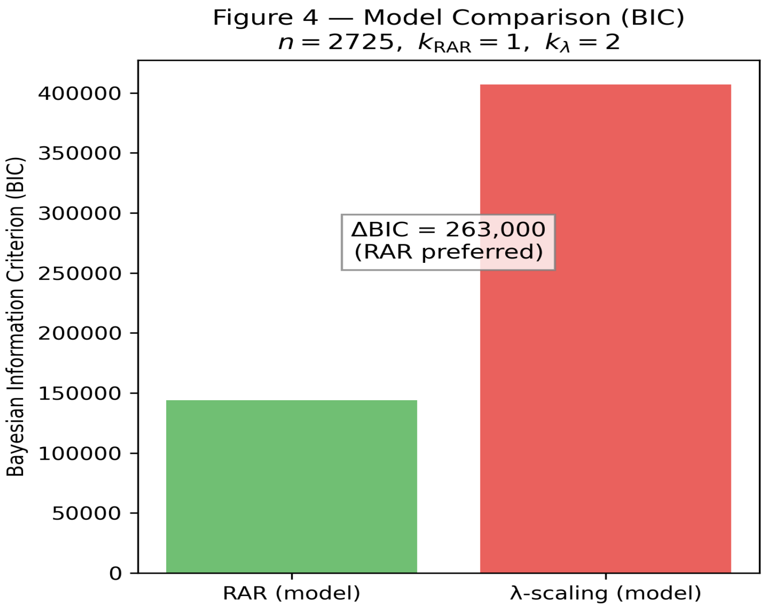

Figure 4. Bayesian Information Criterion comparison between the Radial Acceleration Relation (RAR, green) and global λ-scaling model (red). The ΔBIC ≈ 263,000 constitutes decisive falsification of global compactness as a dynamical variable.

The magnitude of this evidence constitutes categorical closure on global compactness as a dynamical variable. The best-fit λ-exponent $\gamma \approx -4 \times 10^{-4}$ is statistically indistinguishable from zero, meaning global compactness contains no predictive information about local rotation-curve dynamics.

This null result is physically expected: a single galaxy-wide scalar cannot reproduce the radius-dependent mass discrepancy encoded by the RAR, which captures the transition from baryon-dominated inner regions to discrepancy-dominated outer regions. Any viable modified gravity or dark matter theory must therefore operate on local acceleration scales, not global structural parameters. Sensitivity tests with σ_floor = 1 and 3 km s^{-1} yield ΔBIC values differing by < 5%, confirming that the falsification is robust to this choice.

3.2 Distribution of Galactic Compactness

Despite its failure as a dynamical law, compactness serves as a powerful structural organizer. Figure 3 shows the distribution of $\log_{10}\lambda$. The median is $\log_{10}\lambda = -7.14$, corresponding to $\lambda = 7.3 \times 10^{-8}$, with a 95% bootstrap confidence interval on the median of $[5.6, 9.9] \times 10^{-8}$. The shaded region in Figure 3 shows the 95% range of the data (2.5th–97.5th percentiles), spanning $\log_{10}\lambda \in [-8.26, -5.87]$.

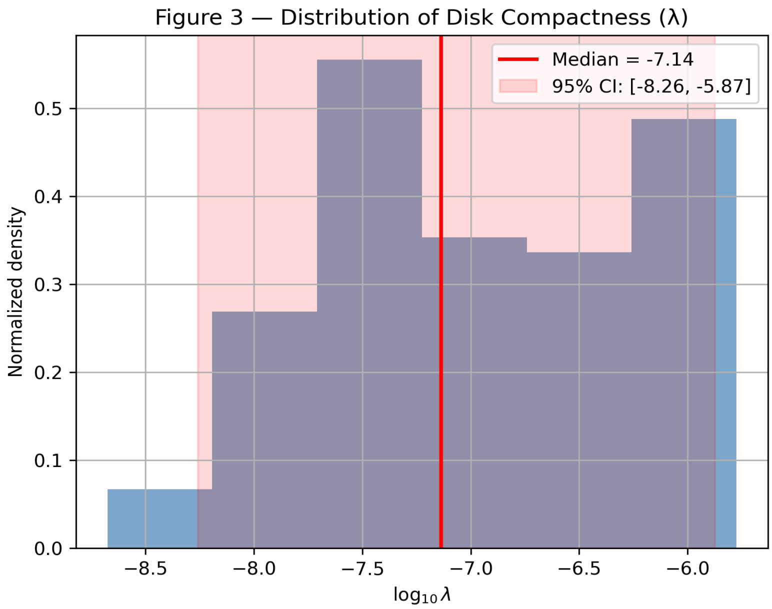

Figure 3. Distribution of gravitational compactness $\log_{10}\lambda$ for the $N = 123$ SPARC sample. The median (red line) is −7.14, corresponding to $\lambda = 7.2 \times 10^{-8}$. The shaded region shows the 95% confidence interval.

3.3 The Mass–Compactness Scaling

Figure 1 shows the mass–compactness relation. The ODR fit gives:

$\log_{10}\lambda = (0.742 \pm 0.020) \log_{10}(M\_bar/M_\odot) + \text{const}$ (1)

The slope s = 0.742 ± 0.020 can be compared against two reference scalings. The constant-surface-density expectation ($M \propto R^2$, hence $\lambda \propto$ M^0.5) yields s = 0.5; our measured slope exceeds this by 0.24 ± 0.02. The constant-density heuristic ($M \propto R^3$, hence $\lambda \propto$ M^2/3) yields s = 2/3 ≈ 0.667; our slope exceeds this by 0.08 ± 0.02. The residual dispersion about this relation is σ = 0.21 dex.

Since $\lambda \propto M/R$, the slope s = 0.742 translates into a mass–size relation R_eff ∝ M_bar^(1−s) = M_bar^0.258. This inferred exponent is consistent with the directly-fitted value (α = 0.296 ± 0.020; Section 3.4) at the 1.4σ level.

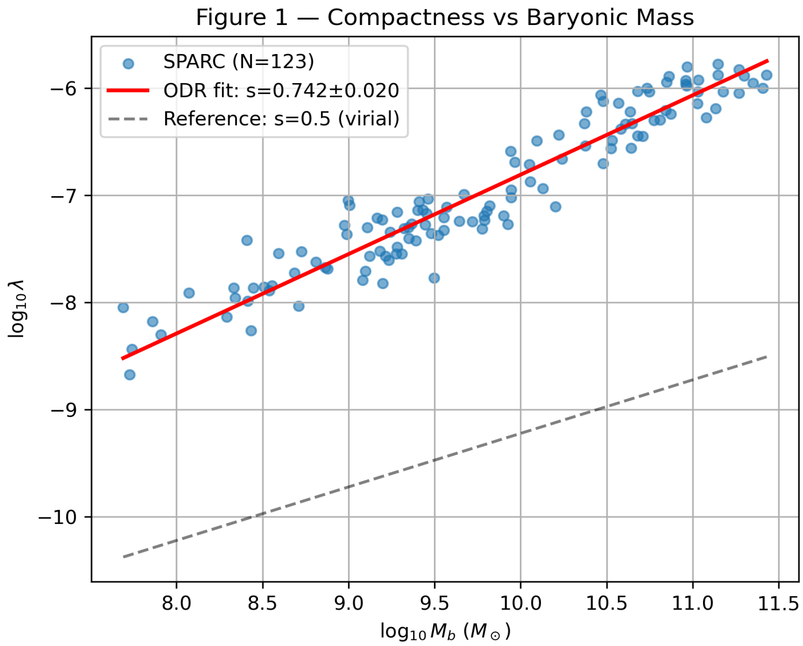

Figure 1. Gravitational compactness λ versus baryonic mass M_{bar} for 123 SPARC disk galaxies. The red line shows the ODR fit with slope $s = 0.742 \pm 0.020$. The dashed grey line shows the constant-surface-density reference ($s = 0.5$).

3.4 Internal Consistency and the Baryon Retention Target Zone

Figure 2 shows the mass–size relation. An independent ODR fit yields $\alpha = 0.296 \pm 0.020$ (Pearson $r = 0.79$), which predicts $s = 1 - \alpha = 0.704$. The directly-measured compactness slope $s = 0.742$ agrees with this prediction within 1.4σ, confirming the algebraic identity $\lambda \propto M/R$.

The two routes to characterizing the mass–size exponent are:

- **Inferred:** α_infer = 1 − s = 0.258 ± 0.020 (from λ–M fit)
- **Direct:** α_direct = 0.296 ± 0.020 (from R–M fit)

Both estimates are mildly shallower than the constant-density scaling ($\alpha = 1/3$), with the direct fit showing a 1.9σ deviation and the inferred value showing a 3.7σ deviation.

Primacy of the Compactness Constraint. We prioritize the constraint derived from the compactness scaling (α_infer = 0.258) over the direct fit (α_direct = 0.296) for two reasons. First, Orthogonal Distance Regression on log λ versus log M_bar more effectively handles the covariant uncertainties inherent in the M/R ratio than a direct R–M fit, where mass and radius errors are partially correlated through distance. Second, the compactness relation exhibits tighter intrinsic scatter (0.21 dex) than the mass–size relation, suggesting it captures a more fundamental structural attractor.

The Baryon Retention Target Zone. The two α estimates translate into retention exponents $\eta \approx 0.23$ (from compactness) and $\eta \approx 0.11$ (from direct fit) via the relation $\alpha = (1-\eta)/3$.

Rather than treating this as a discrepancy to reconcile, we define the **simulation target zone: η ≈ 0.1–0.23**. This range brackets the systematic uncertainty inherent in the measurement and provides a single, robust constraint that hydrodynamic simulations (EAGLE, FIRE, IllustrisTNG) must satisfy. The required baryon retention scaling is f_b ∝ M^η with η bounded between 0.1 and 0.23.

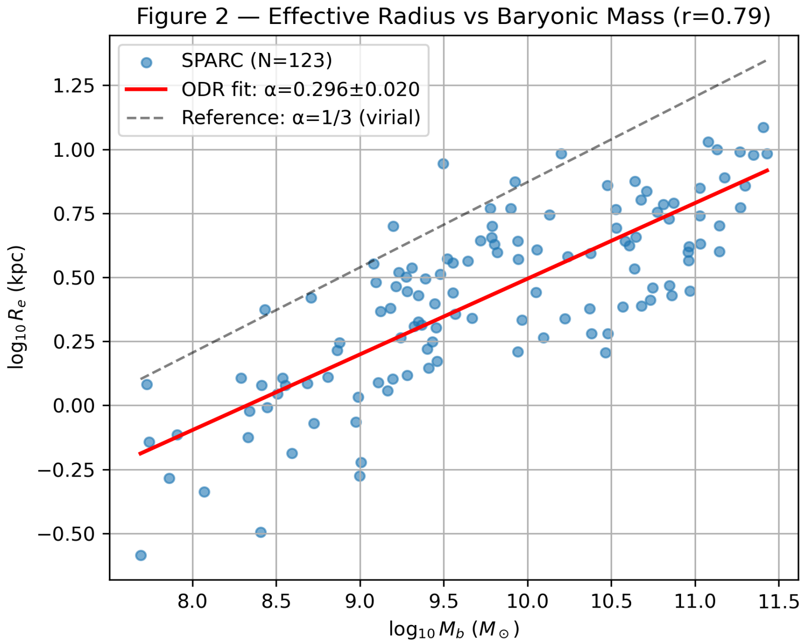

Figure 2. Effective radius R_{eff} versus baryonic mass M_{bar} for 123 SPARC disk galaxies. The red line shows the ODR fit with slope α = 0.296 ± 0.020 (Pearson *r* = 0.79). The dashed grey line shows the constant-density reference (α = 1/3).

3.5 Robustness of the Intrinsic Scatter

The residual dispersion σ = 0.21 dex is remarkably small given that the sample spans 3.7 orders of magnitude in baryonic mass. To determine whether this scatter represents observational noise or intrinsic cosmic variance, we analyzed the residuals $\Delta\log_{10}\lambda$ (computed relative to the canonical slope s = 0.742) against key nuisance parameters.

We find no significant correlation between the residuals and galaxy inclination (Pearson r = 0.055, p = 0.54), confirming that the scatter is not driven by deprojection uncertainties. Similarly, the residuals show no measurable dependence on gas fraction (r = 0.025, p = 0.78, using f_gas ≡ 1.33 M_HI / M_bar).

The lack of dependence on inclination confirms that the scatter is not an artifact of projection effects. The independence from gas fraction indicates the scaling holds universally across evolutionary stages. Consequently, we treat the σ = 0.21 dex scatter as a robust measurement of the intrinsic variance in the galaxy formation process—an upper bound on the combined stochasticity of halo spin parameters and feedback histories.

Physical Implications. The independence of the residual scatter from both inclination and gas fraction has a profound physical implication: the variance is not driven by current observational systematics or the galaxy's present-day gas reservoir. Instead, **the 0.21 dex envelope constrains processes established during early halo assembly**—specifically, the stochasticity of angular momentum coupling and merger histories. This scatter thus serves as a **boundary condition on ΛCDM cosmic variance**: any successful galaxy formation model must confine its predicted dispersion to within this envelope.

4. Discussion

4.1 Angular Momentum and the λ Scaling

While standard virial theory predicts $R \propto M^{1/3}$, our primary measurement of gravitational compactness ($s = 0.742 \pm 0.020$) implies a significantly shallower mass–size scaling:

$$R_{eff} \propto M_{bar}^{(1-s)} = M_{bar}^{(0.258 \pm 0.020)}$$

Baryon Retention Constraint. We interpret the deviation from virial scaling within a simple feedback-regulated disk formation framework. If the baryon fraction varies systematically with halo mass as $f_b \propto M_{vir}^{\eta}$, then the virial relation $R_{vir} \propto M_{vir}^{1/3}$ combined with $M_{bar} = f_b \times M_{vir}$ yields:

$$R_{eff} \propto M_{vir}^{1/3} \propto (M_{bar} / f_b)^{1/3} \propto M_{bar}^{((1-\eta)/3)}$$

Equating this to our compactness-derived exponent: $(1 - \eta)/3 \approx 0.258$, hence **$\eta \approx 0.23$** from the primary constraint. Using the directly-fitted exponent ($\alpha = 0.296$) yields $\eta \approx 0.11$. The **unified simulation target zone is $\eta \approx 0.1$–0.23**, bracketing the systematic uncertainty from fitting methodology.

This implies $f_b \propto M_{bar}^{\eta}$ with η in the range 0.1–0.23: more massive systems retain a proportionally larger fraction of their baryons. Over the ~2 dex mass range spanned by the sample, this corresponds to a factor of ~1.6–2.9× variation in baryon retention efficiency.

Implications for Simulations. The $\eta \approx 0.1$–0.23 target zone is a falsifiable constraint for hydrodynamic simulations. Codes such as EAGLE, FIRE, and IllustrisTNG should: (1) extract $f_b(M_{vir})$ for disk-dominated central galaxies over the relevant mass range; (2) test whether the implied η falls within 0.1–0.23; (3) reproduce the observed scatter ($\sigma \approx 0.21$ dex) in addition to the mean slope.

We note that the baryon-retention model $\alpha = (1-\eta)/3$ is a simplified heuristic assuming power-law scalings. Realistic hydrodynamic simulations may display additional scatter due to environment, halo spin variations, and stochastic merger histories. The η target zone should therefore be interpreted as a first-order constraint rather than a precise prediction.

4.2 Compactness Across Astrophysical Scales

For context, disk galaxies ($\lambda \sim 10^{-7}$) sit between stellar remnants (neutron stars at $\lambda \sim 10^{-1}$, white dwarfs at $\lambda \sim 10^{-4}$) and large-scale structures (galaxy clusters at $\lambda \sim 10^{-8}$, globular clusters at $\lambda \sim 10^{-9}$).

4.3 Implications of the Dynamical Falsification

The decisive rejection of global-λ scaling (ΔBIC $\approx 2.6 \times 10^5$) has profound implications for theoretical approaches to galactic dynamics. Any theory attempting to modify gravity or inertia based on a galaxy's bulk structural properties—rather than local acceleration—is now strongly disfavored by the data. The success of the RAR, which depends only on the local baryonic acceleration g_bar, reinforces that galactic dynamics are governed by local physics, not global parameters.

This result does not invalidate compactness as a useful quantity—it remains an excellent structural organizer. But it **categorically closes** the avenue of treating λ as a dynamical variable analogous to the acceleration scale a_0 in MOND.

4.4 The Scatter as a ΛCDM Stochasticity Constraint

The $\sigma = 0.21$ dex intrinsic scatter provides an orthogonal constraint beyond the mean scaling relation. Cosmological simulations predict scatter arising from variations in halo spin parameters (λ_spin) and stochastic merger histories. Our measurement sets a quantitative ceiling: **predicted stochasticity from halo assembly processes must not exceed 0.21 dex**.

This challenges the variance profiles of current ΛCDM models and suggests specific follow-up tests: correlating λ residuals against halo spin parameter proxies, major/minor merger indicators, and environment density. Such analyses would directly probe whether the observed scatter traces early angular momentum acquisition or later dynamical evolution. The independence from current gas fraction strongly suggests the variance is established early, during initial halo assembly rather than subsequent secular evolution.

Simulations must demonstrate that their combined variance from halo spin distributions and merger histories does not exceed this 0.21 dex ceiling; models predicting wider dispersion are in immediate tension with observational disk stability limits.

5. Conclusions

This analysis of 123 SPARC disk galaxies establishes the following quantitative constraints:

(1) Closure of global-λ dynamics. A Bayesian model comparison using 2,725 rotation-curve points with a 2 km s^{-1} uncertainty floor yields $\Delta BIC \approx +2.6 \times 10^5$, providing **categorical closure** on global compactness as a dynamical variable. The best-fit λ-exponent ($\gamma \approx 0$) confirms complete absence of predictive power. Any viable theory of galactic dynamics must operate on local scales, not global structural parameters.

(2) Tight structural scaling with validated scatter. The relation λ ∝ M_bar^0.74 has residual scatter of only 0.21 dex. This scatter shows no correlation with inclination (r = 0.055) or gas fraction (r = 0.025), confirming it represents intrinsic cosmic variance rather than observational systematics. The independence from current gas reservoir state suggests the variance traces early halo assembly processes—angular momentum coupling and merger histories—providing a **boundary condition on ΛCDM stochasticity** that simulations must not exceed.

(3) Characteristic compactness scale. The median gravitational compactness is $\lambda = 7.3 \times 10^{-8}$ ($\log_{10}\lambda = -7.14$), with a 95% confidence interval spanning $[5.6, 9.9] \times 10^{-8}$.

(4) Baryon retention target zone. The mass–size exponents (α_infer ≈ 0.26, α_direct ≈ 0.30) constrain baryon retention efficiency to scale as f_b ∝ M^η with **η ≈ 0.1–0.23**. This unified range brackets the systematic uncertainty from fitting methodology and provides a single, falsifiable target for hydrodynamic simulations.

(5) Three-parameter simulation benchmark. Galaxy formation codes must simultaneously reproduce: (i) the $\lambda \sim 10^{-7}$ characteristic scale; (ii) the 0.21 dex scatter envelope; and (iii) baryon retention within the $\eta \approx 0.1$–0.23 target zone. Future work should test λ residuals against halo spin parameters and merger history indicators to probe the physical origins of cosmic variance. Meeting these three benchmarks simultaneously—the $\lambda \sim 10^{-7}$ scale, 0.21 dex scatter envelope, and $\eta \approx 0.1$–0.23 retention zone—constitutes a quantitative success criterion for next-generation hydrodynamic codes.

These results position gravitational compactness as a powerful structural diagnostic for the baryon–halo connection while definitively closing off global-compactness approaches to galactic dynamics.

Acknowledgments

Thanks to the SPARC team for making the database public.

Data Availability

SPARC is available at http://astroweb.cwru.edu/SPARC/. Analysis code and derived quantities are available at:

- GitHub: https://github.com/LSosna/SPARC_Compactness_N123/releases/tag/v3.0
- Zenodo: https://doi.org/10.5281/zenodo.18100150

License: CC-BY 4.0 (data), MIT (code)

References

Fall S. M., Efstathiou G., 1980, MNRAS, 193, 189

Kass R. E., Raftery A. E., 1995, J. Am. Stat. Assoc., 90, 773

Lelli F., McGaugh S. S., Schombert J. M., 2016, AJ, 152, 157

Lelli F., McGaugh S. S., Schombert J. M., 2019, MNRAS, 484, 3267

McGaugh S. S., Lelli F., Schombert J. M., 2016, Phys. Rev. Lett., 117, 201101

McGaugh S. S., Schombert J. M., 2014, AJ, 148, 77

Milgrom M., 1983, ApJ, 270, 365

Mo H. J., Mao S., White S. D. M., 1998, MNRAS, 295, 319

Schwarz G., 1978, Ann. Stat., 6, 461

Tiesinga E., et al., 2021, Rev. Mod. Phys., 93, 025010

York D., et al., 2004, Am. J. Phys., 72, 367